IEEE Access
Multidisciplinary | Rapid Review | Open Access Journal

Received June 28, 2019, accepted July 16, 2019, date of publication July 19, 2019, date of current version August 7, 2019.

Digital Object Identifier 10.1109/ACCESS.2019.2930029

An Adaptive Approach for the Joint Antenna Selection and Beamforming Optimization

GUILHERME MARTIGNAGO ZILLI[1], (Student Member, IEEE), CIRO ANDRÉ PITZ[2], EDUARDO LUIZ ORTIZ BATISTA[2], (Member, IEEE), RUI SEARA[2], (Senior Member, IEEE), AND WEI-PING ZHU[1], (Senior Member, IEEE)

[1]Department of Electrical and Computer Engineering, Concordia University, Montreal, QC H3G 1M8, Canada
[2]LINSE–Circuits and Signal Processing Laboratory, Department of Electrical Engineering, Federal University of Santa Catarina, Florianópolis 88040-900, Brazil

Corresponding author: Guilherme Martignago Zilli (guilherme.m.zilli@gmail.com)

This work was supported in part by the Brazilian National Council for Scientific and Technological Development (CNPq), in part by the Fonds de Recherche du Québec—Nature et Technologies (FRQNT), and in part by the Natural Sciences and Engineering Research Council (NSERC) of Canada.

ABSTRACT Adaptive beamforming techniques are widely known for their capability of leveraging the performance of antenna arrays. The effectiveness of such techniques typically increases as the number of antennas grows. In contrast, computational and hardware costs very often limit the deployment of beamforming in large-scale arrays. To circumvent this problem, antenna selection strategies have been developed aiming to maintain much of the performance gain obtained by using a large array while keeping computational and hardware costs at acceptable levels. In this context, the present paper is dedicated to the development of two new adaptive algorithms for solving the problem of joint antenna selection and beamforming for uplink reception in mobile communication systems. Both algorithms are based on an alternating optimization strategy and are designed to operate with a limited number of radio-frequency chains. The main difference between the proposed algorithms is that the first is formulated by considering the minimum mean-square error (MMSE) criterion, while the second is based on the minimum-variance distortionless-response (MVDR) approach. The numerical simulation results confirm the effectiveness of the proposed algorithms.

INDEX TERMS Adaptive arrays, antenna selection, beamforming, MMSE criterion, MVDR criterion.

I. INTRODUCTION

Smart antennas have been considered as promising solutions to several problems of cellular communication systems, such as, limited spectrum availability; reduced battery life of mobile devices; interference due to frequency reuse; and time and frequency selective fading [1], [2]. The term smart antenna in fact refers to the structure formed by an antenna array along with a digital signal processing hardware that implements a spatial filtering (beamforming) algorithm. Such an arrangement allows a dynamic real-time adjustment of the radiation pattern without structural changes [3]. Due to hardware limitations, smart antennas are generally located at the base station (BS) of cellular communication systems, while the multiple mobile stations (MSs) are kept with a single or very few antennas.

The associate editor coordinating the review of this manuscript and approving it for publication was Liangtian Wan.

The performance gain obtained by using smart antennas gets larger as the number of array elements increases [1]. Such a characteristic has motivated the development of large-scale arrays, the so-called massive multiple-input multiple-output (MIMO) [4]. However, implementation costs often limit the expansion of the number of antennas in massive MIMO arrays. This problem is especially relevant in mmWave communication systems, in which the very high carrier frequencies and signal bandwidths result in severe hardware constraints [5]. Although the cost of additional antenna elements and the associated signal processing hardware is relatively small, the high cost of radio frequency (RF) chains (comprising amplifiers, filters, frequency converters, analog-to-digital and digital-to-analog converters, among others) restricts the implementation of mmWave communication systems with a higher number of antennas [6]–[8]. Furthermore, it is well known that, in a real-world propagation environment, the elements of an antenna array do not

contribute equally to the overall system performance [9]. In this context, several strategies have been devised in order to efficiently allocate the available RF chains, such as the use of coprime arrays [10] or antenna selection techniques [6]–[9]. In particular, antenna selection has gained considerable attention in mmWave massive MIMO as it has been used in conjunction with or as alternative to hybrid beamforming, allowing to reduce both hardware complexity and power consumption [11]–[14].

Antenna selection techniques account for finding the optimal subset of antennas within the available set. Solving this problem is not a trivial task, since it, in general, involves an extensive search within all possible combinations of antennas, making the problem computationally prohibitive even for arrays with a few dozens of elements [7], [8]. As a result, several suboptimal strategies have been proposed in the literature aiming to solve antenna-selection problems. For instance, in [15], a decremental antenna-selection scheme is introduced by using a capacity-maximization criterion for iteratively removing antenna elements until a desired number of antennas is reached. By exploiting a similar concept, an incremental antenna-selection technique is proposed in [16], where the antenna elements are iteratively included. Despite their conceptual simplicity, these techniques assume time-invariant channel state information and also require the evaluation of capacity loss/gain for every removed/included antenna. The resulting computational costs limit the application of these techniques especially in large-scale arrays and non-stationary environments. In [17], receive antenna selection is cast as a capacity-maximization-based convex problem that can be solved in polynomial time. The obtained solution is, however, channel dependent, which restrains the application of this method to stationary environments. Convex optimization has also been applied to antenna selection aiming to minimize the mean-square error (MSE) [18] and to maximize the channel capacity in massively distributed antenna systems [19]. The main drawback of these approaches is their reliance on computationally costly optimization solvers, usually with computational complexity in the order of $\mathcal{O}(M^3)$ (where M is the number of antennas) [20], which makes a real-time implementation very hard.

In [21] and [22], adaptive antenna selection algorithms based on stochastic optimization are proposed in order to maximize both the channel capacity and the signal-to-noise ratio (SNR), and minimize the bit error rate. These algorithms are focused on real-time operation and are capable of tracking a suboptimal antenna subset in time-varying channels. However, such algorithms not only require a dictionary containing all possible combinations of antenna selection along with their corresponding probabilities, but also require the computation of the cost function twice in each iteration [21], [22]. As a consequence, the algorithms in [21] and [22] require a large amount of memory and high computational complexity.

The approaches proposed in [15]–[19], [21], and [22] consider the antenna selection problem apart from the beamforming design. In contrast, joint antenna selection and beamforming (JASB) problems have been the subject of several other research works [23]–[30]. Transmit JASB problems can be formulated under different criteria, such as total power minimization under quality-of-service (QoS) constraints [23], [24], energy-efficiency maximization [25], and decremental selection based on power minimization [26]. These problems involve, in general, solving one or multiple semidefinite programming (SDP) problems, and therefore, also rely on computationally costly optimization solvers.

On the other hand, several low-complexity adaptive techniques have been proposed for solving receive JASB problems. For instance, the adaptive algorithms proposed in [27]–[30] indirectly promote antenna selection by inserting sparsity-inducing ℓ_1-norm or ℓ_0-norm constraints into the derivation of constrained least-mean-square (CLMS) algorithms [30]–[32]. In doing so, antenna selection can be performed by thinning the array, i.e., by switching off the antenna elements for which the beamforming coefficients are very small [27]. Such an approach is useful when the aim is to reduce power consumption and heat dissipation [30]. However, one common assumption for the development of the algorithms in [27]–[30] is that the signal received by each antenna element is available at every iteration of the adaptive process, which does not comply with physical limitations on the number of RF chains.

The goal of this paper is to fill an important gap in the context of JASB problems, which is the lack of adaptive algorithms capable of dealing with fixed limits on the number of RF chains. In particular, we focus on the development of two new adaptive algorithms to solve receive JASB problems in cellular systems. These algorithms are based on an alternating optimization strategy [33] that searches for the optimal solution by performing two steps at every algorithm iteration: first the beamforming vector is obtained by considering an *a priori* antenna selection, and then the antenna selection is updated using the *a posteriori* beamforming vector. The proposed algorithms are capable of attaining high levels of signal-to-interference-plus-noise ratio (SINR), while strictly complying with limitations on the number of RF chains. Moreover, the proposed algorithms can track channel changes, making them suitable for operation in non-stationary environments, requiring only information about the desired signal (i.e., the corresponding direction of arrival or a reference signal).

The main contributions of this paper are described in the following:

- We propose a novel adaptive JASB algorithm (AJASB) based on the minimum MSE (MMSE) criterion. The idea behind such an algorithm is to compute both the beamforming vector and the antenna selection aiming to reduce the MSE. In this context, the beamforming problem is formulated as an unconstrained MSE minimization problem and the beamforming vector is updated by means of the normalized least-mean-square (NLMS) algorithm. In addition, the antenna selection problem is formulated as a constrained MSE minimization problem

(taking into account the hardware limitations) and the antenna selection is updated by using a constrained NLMS (CNLMS)-based algorithm.
- We also propose a second AJASB algorithm based on the minimum-variance distortionless-response (MVDR) approach. In this algorithm, the beamforming vector is obtained from the MVDR problem, i.e., by minimizing the variance at the output of the beamformer, while maintaining a constant gain toward the desired user. Similarly, the MVDR approach is used along with an additional constraint on the number of available RF chains to formulate the antenna selection problem. Both the beamforming vector and the antenna selection are updated by using CNLMS-based algorithms.
- We further provide extensive simulation results to assess the performance of the proposed algorithms under different scenarios.

The paper is organized as follows. We start by presenting the system model and the problem statement in Section II. In Sections III and IV, we propose new strategies for solving the MMSE-based and the MVDR-based JASB problems, respectively. In Section V, simulation results for different operating scenarios are presented aiming to assess and compare the proposed algorithms for performance. Finally, concluding remarks are given in Section VI.

Throughout the paper, we adopt the following notations: non-bold letters, either lower or upper case, are used for scalars; boldfaced lower-case letters are used for vectors; and boldfaced upper-case letters are used for matrices. The M-dimensional identity matrix is denoted by $\mathbf{I}_{\mathrm{M}}$ and the $M \times N$ matrix of zeros is denoted by $\mathbf{0}_{M\times N}$, while $\mathbf{0}$ and $\mathbf{1}$ represent, respectively, vectors of zeros and ones. The operators $(\cdot)^*$, $(\cdot)^{\mathrm{T}}$, and $(\cdot)^{\mathrm{H}}$ denote, respectively, the complex conjugate, the transpose, and the Hermitian (or conjugate transpose). The matrix trace, the expectation, and the real-part operator are denoted by $\mathrm{Tr}\,(\cdot)$, $\mathrm{E}\,(\cdot)$, and $\mathrm{Re}\,(\cdot)$, respectively.

II. SYSTEM MODEL AND PROBLEM STATEMENT

In this section, the communication scenario considered in this work is firstly depicted, followed by the description of the adopted performance metric, and the optimization problem that lays the groundwork for developing the proposed algorithms.

A. SCENARIO DEFINITION

The scenario considered in this work involves a multi-cell cellular system in which each BS serves multiple single-antenna users. For a particular BS, we assume that the intra-cell users are allocated to different channel resources and therefore, do not interfere each other. On the other hand, $K-1$ inter-cell users located at nearby cells share the same channel resources with a given intra-cell user, as illustrated in Fig. 1. Moreover, we assume that the considered BS is equipped with a massive antenna array. Such array is partitioned into subarrays formed by M-element antenna and $L \leq M$ RF

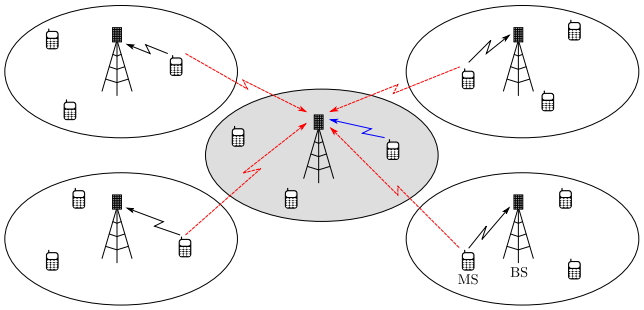

FIGURE 1. Multi-cell system configuration with the signal of interest (blue line) and the interfering signals (red lines) arriving at the considered BS.

chains, where the subarrays are individually assigned to each intra-cell user [12]–[14].

The uplink signals arriving at the subarray allocated to a given intra-cell user are arranged in the input vector $\mathbf{x}(n) \in \mathbb{C}^{M\times 1}$, which is modeled by using an equivalent baseband representation as

$$\mathbf{x}(n) = \sum_{i=0}^{K-1} \mathbf{a}(\theta_i)\beta_i(n) + \mathbf{z}(n) \tag{1}$$

where $\mathbf{a}(\theta_i) \in \mathbb{C}^{M\times 1}$ represents the steering vector related to the angle of arrival θ_i of the ith user; the complex scalar $\beta_i(n)$ denotes the baseband symbol with zero mean and power $p_i = \mathrm{E}[|\beta_i(n)|^2]$ corresponding to the ith user; and $\mathbf{z}(n) \in \mathbb{C}^{M\times 1}$ models the complex additive white Gaussian noise (AWGN) with power σ_z^2 present at each antenna element. Note that the signals transmitted by the remaining intra-cell users are not considered in (1), since they are allocated to different channel resources.

The input vector after the antenna selection, which contains the signals processed by the RF chains, can be written as

$$\mathbf{x}_{\mathrm{s}}(n) = \mathbf{S}\mathbf{x}(n) \tag{2}$$

with $\mathbf{S}$ representing an $M \times M$ diagonal antenna-selection matrix $\mathbf{S}$ whose mth diagonal element is given by

$$[\mathbf{S}]_{m,m} = \begin{cases} 1, & \text{if the } m\text{th antenna is selected} \\ 0, & \text{if the } m\text{th antenna is not selected.} \end{cases}$$

Note that, in practice, only $\mathbf{x}_{\mathrm{s}}(n)$ is available for the system. Now, considering the number of selected antennas equal to the number of available RF chains, we have $\mathrm{Tr}\,(\mathbf{S}) = L$. In particular, when all antennas are selected (i.e., $L = M$), $\mathbf{S}$ becomes the $M \times M$ identity matrix $\mathbf{I}_M$, resulting in $\mathbf{x}_{\mathrm{s}}(n) = \mathbf{x}(n)$.

Denoting $\mathbf{w} \in \mathbb{C}^{M\times 1}$ as the beamforming vector, the output of the beamformer can be written as

$$y(n) = \mathbf{w}^{\mathrm{H}}\mathbf{x}_{\mathrm{s}}(n). \tag{3}$$

Furthermore, defining the first inter-cell user ($i = 0$) as the signal of interest (SOI), the reference signal becomes $d(n) = \beta_0(n)$, and the error signal between such a reference signal and the beamformer output can be defined as

$$e(n) = d(n) - y(n) = \beta_0(n) - \mathbf{w}^{\mathrm{H}}\mathbf{x}_{\mathrm{s}}(n). \tag{4}$$

Next, using (2), (3), and (4), the MSE is given as

$$\begin{aligned}\mathrm{E}\left[|e(n)|^2\right] &= \mathrm{E}\left\{[\beta_0(n) - y(n)][\beta_0^*(n) - y^*(n)]\right\} \\ &= \mathbf{w}^{\mathrm{H}}\mathbf{S}\mathbf{R}_{\mathbf{x}}\mathbf{S}\mathbf{w} - 2\mathrm{Re}(\mathbf{w}^{\mathrm{H}}\mathbf{S}\mathbf{p}) + p_0^2 \end{aligned} \tag{5}$$

where $\mathbf{R}_{\mathrm{x}} = \mathrm{E}\left[\mathbf{x}(n)\mathbf{x}^{\mathrm{H}}(n)\right]$ denotes the autocorrelation matrix of the input vector, and $\mathbf{p} = \mathrm{E}\left[\mathbf{x}(n)\beta_0^*(n)\right]$ is the cross-correlation vector between the input vector and the complex conjugate of the desired signal.

To obtain an expression for the SINR at the beamformer output, the mean power (variance) of $y(n)$ is derived from (3) as follows:

$$\mathrm{E}\left[|y(n)|^2\right] = \mathbf{w}^{\mathrm{H}}\mathbf{S}\mathbf{R}_{\mathrm{x}}\mathbf{S}\mathbf{w}. \tag{6}$$

If we further assume that the baseband symbols are independent, i.e., $\mathrm{E}[\beta_i(n)\beta_j^*(n)] = 0$ for $i \neq j$, $\mathbf{R}_{\mathrm{x}}$ can be expressed as

$$\mathbf{R}_{\mathrm{x}} = \sum_{i=0}^{K-1} p_i \mathbf{a}(\theta_i)\mathbf{a}^{\mathrm{H}}(\theta_i) + \sigma_z^2 \mathbf{I}_M. \tag{7}$$

Then, rearranging (7) into

$$\mathbf{R}_{\mathrm{x}} = \mathbf{R}_{\mathrm{soi}} + \mathbf{R}_{\mathrm{in}} \tag{8}$$

with

$$\mathbf{R}_{\mathrm{soi}} = p_0 \mathbf{a}(\theta_0)\mathbf{a}^{\mathrm{H}}(\theta_0) \tag{9}$$

representing the autocorrelation matrix of the SOI and

$$\mathbf{R}_{\mathrm{in}} = \sum_{i=1}^{K-1} p_i \mathbf{a}(\theta_i)\mathbf{a}^{\mathrm{H}}(\theta_i) + \sigma_z^2 \mathbf{I}_M \tag{10}$$

the autocorrelation matrix of the interference plus noise, (6) can be rewritten as

$$\mathrm{E}\left[|y(n)|^2\right] = \mathbf{w}^{\mathrm{H}}\mathbf{S}\mathbf{R}_{\mathrm{soi}}\mathbf{S}\mathbf{w} + \mathbf{w}^{\mathrm{H}}\mathbf{S}\mathbf{R}_{\mathrm{in}}\mathbf{S}\mathbf{w}. \tag{11}$$

Thus, the SINR at the beamformer output is given by

$$\gamma = \frac{\mathbf{w}^{\mathrm{H}}\mathbf{S}\mathbf{R}_{\mathrm{soi}}\mathbf{S}\mathbf{w}}{\mathbf{w}^{\mathrm{H}}\mathbf{S}\mathbf{R}_{\mathrm{in}}\mathbf{S}\mathbf{w}}. \tag{12}$$

B. JOINT ANTENNA SELECTION AND BEAMFORMING PROBLEM

In order to address the joint antenna selection and beamforming problem with a limited number of RF chains, the idea here is to optimize some performance metric $\Phi(\mathbf{w}, \mathbf{S})$ subject to a constraint on the number of selected antennas. As a result, we have the following constrained optimization problem:

$$\begin{aligned} &\underset{\mathbf{w},\mathbf{S}}{\text{minimize}}\ \Phi(\mathbf{w}, \mathbf{S}) \\ &\text{subject to}\ [\mathbf{S}]_{m,m} \in \{0,\ 1\} \\ &\qquad\qquad \mathrm{Tr}\,(\mathbf{S}) = L. \end{aligned} \tag{13}$$

In this paper, we particularly focus on two criteria for choosing $\Phi(\mathbf{w}, \mathbf{S})$: MMSE and MVDR. It is noteworthy that regardless of the choice of $\Phi(\mathbf{w}, \mathbf{S})$, the problem in (13) is NP-hard due to the binary constraints involved [8], [17]. Therefore, finding an optimal solution to (13) is very computationally expensive, especially for large scale arrays [8].

It is important to notice that a single SOI is considered in (13) due to the assumption that an individual subarray is allocated for each intra-cell user. In cases where the intra-cell users share the same channel and/or RF hardware resources, the objective function of (13) must be reformulated in order to include all intra-cell users. However, such an extension is out of the scope of this paper and is left as a suggestion for future works.

III. MMSE-BASED ADAPTIVE JOINT ANTENNA SELECTION AND BEAMFORMING

This section is focused on the development of a new MMSE-based adaptive algorithm for solving (13). To this end, we assume $\Phi(\mathbf{w}, \mathbf{S}) = \mathrm{E}\left[|e(n)|^2\right]$ and partition (13) in such a way that $\mathbf{w}$ and $\mathbf{S}$ can be obtained by using an alternating optimization approach. In this context, we start by formulating the MMSE problem considering a fixed antenna-selection scenario aiming to obtain $\mathbf{w}$. Next, a new strategy for antenna selection is proposed, allowing us to obtain $\mathbf{S}$.

A. MMSE BEAMFORMING

The beamforming procedure considered in this section is based on the minimization of $\mathrm{E}\left[|e(n)|^2\right]$ as defined in (5). Thus, the beamforming vector is obtained from the following optimization problem:

$$\underset{\mathbf{w}}{\text{minimize}}\quad \mathbf{w}^{\mathrm{H}}\mathbf{S}\mathbf{R}_{\mathbf{x}}\mathbf{S}\mathbf{w} - 2\mathrm{Re}(\mathbf{w}^{\mathrm{H}}\mathbf{S}\mathbf{p}) + p_0^2. \tag{14}$$

The optimum solution for (14) is the well-known Wiener-Hopf solution [34], i.e.,

$$\mathbf{w}_{\mathrm{o}} = (\mathbf{S}\mathbf{R}_{\mathbf{x}}\mathbf{S})^{\dagger}\mathbf{S}\mathbf{p} \tag{15}$$

where $\mathbf{w}_{\mathrm{o}}$ represents the optimum beamforming vector and $(\cdot)^{\dagger}$ denotes the Moore-Penrose inverse, which is required since $\mathbf{S}\mathbf{R}_{\mathbf{x}}\mathbf{S}$ results in a rank-deficient matrix [i.e., $\mathrm{rank}(\mathbf{S}\mathbf{R}_{\mathbf{x}}\mathbf{S}) = L \leq M$]. One can notice from (15) that the evaluation of the Wiener-Hopf solution requires not only the *a priori* knowledge of $\mathbf{R}_{\mathrm{x}}$ and $\mathbf{p}$, but also the computation of $(\mathbf{S}\mathbf{R}_{\mathbf{x}}\mathbf{S})^{\dagger}$. This results in a high computational burden, especially in cases involving real-time processing, massive arrays and/or non-stationary scenarios. Therefore, to overcome these difficulties, the steepest descent method [34] is used for iteratively obtaining the beamforming vector, which leads to the following update rule:

$$\begin{aligned}\mathbf{w}(n+1) &= \mathbf{w}(n) - \mu_{\mathrm{w}}\nabla_{\mathrm{w}^*}\mathrm{E}\left[|e(n)|^2\right] \\ &= \mathbf{w}(n) - \mu_{\mathrm{w}}\left[\mathbf{S}\mathbf{R}_{\mathbf{x}}\mathbf{S}\mathbf{w}(n) - \mathbf{S}\mathbf{p}\right]. \end{aligned} \tag{16}$$

with $\nabla_{\mathrm{w}^*}\mathrm{E}\left[|e(n)|^2\right] = \left[\mathbf{S}\mathbf{R}_{\mathbf{x}}\mathbf{S}\mathbf{w}(n) - \mathbf{S}\mathbf{p}\right]$ representing the gradient of $\mathrm{E}\left[|e(n)|^2\right]$ with respect to the complex conjugate of $\mathbf{w}$. Then, considering (2)-(4) and replacing $\mathbf{R}_{\mathbf{x}}$ and $\mathbf{p}$ by the corresponding instantaneous estimates given, respectively, by $\mathbf{x}(n)\mathbf{x}^{\mathrm{H}}(n)$ and $\mathbf{x}(n)\beta_0^*(n)$, we obtain an LMS-type update

expression, which is given by

$$\begin{aligned}\mathbf{w}(n+1) &= \mathbf{w}(n) - \mu_{\mathrm{w}}\left[\mathbf{x}_{\mathrm{s}}(n)\mathbf{x}_{\mathrm{s}}^{\mathrm{H}}(n)\mathbf{w}(n) - \mathbf{x}_{\mathrm{s}}(n)\beta_0^*(n)\right] \\ &= \mathbf{w}(n) + \mu_{\mathrm{w}}\mathbf{x}_{\mathrm{s}}(n)e^*(n) \end{aligned} \tag{17}$$

where μ_{w} is the step-size parameter. It is important to highlight that only the input signals present at the selected antennas are used in (17), and therefore, only the coefficients corresponding to these antennas are updated at a given iteration. As a consequence, the hardware constraint of number of available RF chains is fulfilled and the computational complexity of the algorithm is reduced. Moreover, we assume that the error signal $e(n)$ required by (17) is obtained during a training period, wherein the intra-cell users transmit a predefined training sequence (reference signal) known to the BS. The design of this training sequence, including its length and repetition rate, directly impact the ability of the system to track channel variations, thereby influencing the performance of the AJASB algorithm. However, such a design is out of the scope of this paper, being a recurrent research topic available in the open literature (see [35]–[38], for example).

Finally, to achieve a faster convergence and easier parameter adjustment, a normalized version of (17) is also formulated here following the same idea used for developing the NLMS algorithm [34]. Thus, the following NLMS update rule is obtained:

$$\mathbf{w}(n+1) = \mathbf{w}(n) + \mu_{\mathrm{w}}\frac{\mathbf{x}_{\mathrm{s}}(n)e^*(n)}{\mathbf{x}_{\mathrm{s}}^{\mathrm{H}}(n)\mathbf{x}_{\mathrm{s}}(n) + \varepsilon} \tag{18}$$

with ε representing a regularization term that has been included in (18) to prevent divisions by very small values [34].

B. MMSE ANTENNA SELECTION

The MMSE antenna selection problem considered here consists of finding the antenna subset that minimizes (5). This problem can be mathematically described as

$$\begin{aligned} &\underset{\mathbf{S}}{\text{minimize}}\ \mathbf{w}^{\mathrm{H}}\mathbf{S}\mathbf{R}_{\mathbf{x}}\mathbf{S}\mathbf{w} - 2\mathrm{Re}\{\mathbf{w}^{\mathrm{H}}\mathbf{S}\mathbf{p}\} + p_0^2 \\ &\text{subject to}\ \ [\mathbf{S}]_{m,m} \in \{0,\ 1\} \\ &\qquad\qquad \mathrm{Tr}\,(\mathbf{S}) = L. \end{aligned} \tag{19}$$

In spite of being easier to solve it in comparison to (13) (since only $\mathbf{S}$ needs to be optimized), (19) is still an NP-hard problem due to the binary constraints involved. To circumvent this drawback, we relax the binary constraints allowing $[\mathbf{S}]_{m,m}$ to be a real number. Then, defining the auxiliary vector $\mathbf{s}$ as the diagonal vector of $\mathbf{S}$, defining also $\mathbf{W}$ as a diagonal matrix whose entries are given by $\mathbf{w}$ [i.e., $\mathbf{W} = \mathrm{diag}(\mathbf{w})$], and considering that p_0^2 does not depend on the optimization variable, the relaxed version of (19) becomes

$$\begin{aligned} &\underset{\mathbf{s}\in\mathbb{R}^M}{\text{minimize}}\ \mathbf{s}^{\mathrm{T}}\mathbf{W}^{\mathrm{H}}\mathbf{R}_{\mathbf{x}}\mathbf{W}\mathbf{s} - 2\mathrm{Re}\{\mathbf{s}^{\mathrm{T}}\mathbf{W}^{\mathrm{H}}\mathbf{p}\} \\ &\text{subject to}\ \mathbf{1}^{\mathrm{T}}\mathbf{s} = L. \end{aligned} \tag{20}$$

Note that $\mathbf{W}^{\mathrm{H}}\mathbf{R}_{\mathbf{x}}\mathbf{W}$ is a positive semidefinite matrix and, therefore, (20) is a convex problem [39].

To find the optimal solution for (20), we first write its Lagrangian as

$$\mathcal{L}(\mathbf{s},\lambda) = \mathbf{s}^{\mathrm{T}}\mathbf{W}^{\mathrm{H}}\mathbf{R}_{\mathbf{x}}\mathbf{W}\mathbf{s} - 2\mathbf{s}^{\mathrm{T}}\mathrm{Re}\{\mathbf{W}^{\mathrm{H}}\mathbf{p}\} + \lambda(\mathbf{1}^{\mathrm{T}}\mathbf{s} - L) \tag{21}$$

where λ is the Lagrange multiplier. Next, we take the gradient of (21) with respect to $\mathbf{s}$, resulting in

$$\nabla_{\mathbf{s}}\mathcal{L}(\mathbf{s},\lambda) = 2\mathbf{R}_{\mathrm{rw}}\mathbf{s} - 2\mathbf{r}_p + \lambda\mathbf{1} \tag{22}$$

with

$$\mathbf{R}_{\mathrm{rw}} = \mathrm{Re}\{\mathbf{W}^{\mathrm{H}}\mathbf{R}_{\mathbf{x}}\mathbf{W}\} \tag{23}$$

and

$$\mathbf{r}_{\mathrm{p}} = \mathrm{Re}\{\mathbf{W}^{\mathrm{H}}\mathbf{p}\}. \tag{24}$$

The optimum selection vector $\mathbf{s}_{\mathrm{o}}$ is obtained by solving $\nabla_{\mathbf{s}}\mathcal{L}(\mathbf{s},\lambda) = \mathbf{0}$, which leads to

$$\mathbf{s}_{\mathrm{o}} = \frac{1}{2}\mathbf{R}_{\mathrm{rw}}^{-1}\left(2\mathbf{r}_{\mathrm{p}} - \lambda\mathbf{1}\right). \tag{25}$$

Regarding λ, its value is obtained by reinforcing the constraint $\mathbf{1}^{\mathrm{T}}\mathbf{s}_{\mathrm{o}} = L$. Then, pre-multiplying both sides of (25) by $\mathbf{1}^{\mathrm{T}}$ and manipulating the resulting expression, we get

$$\lambda = 2\left[\frac{\mathbf{1}^{\mathrm{T}}\mathbf{R}_{\mathrm{rw}}^{-1}\mathbf{r}_p - L}{\mathbf{1}^{\mathrm{T}}\mathbf{R}_{\mathrm{rw}}^{-1}\mathbf{1}}\right]. \tag{26}$$

Next, substituting (26) into (25), we obtain

$$\mathbf{s}_{\mathrm{o}} = \mathbf{R}_{\mathrm{rw}}^{-1}\mathbf{r}_{\mathrm{p}} - \frac{\mathbf{R}_{\mathrm{rw}}^{-1}(\mathbf{1}^{\mathrm{T}}\mathbf{R}_{\mathrm{rw}}^{-1}\mathbf{r}_{\mathrm{p}})\mathbf{1}}{\mathbf{1}^{\mathrm{T}}\mathbf{R}_{\mathrm{rw}}^{-1}\mathbf{1}} + L\frac{\mathbf{R}_{\mathrm{rw}}^{-1}\mathbf{1}}{\mathbf{1}^{\mathrm{T}}\mathbf{R}_{\mathrm{rw}}^{-1}\mathbf{1}}. \tag{27}$$

Note that $\mathbf{s}_{\mathrm{o}}$ is a vector of real numbers and, thus, the diagonal elements of the antenna-selection matrix $\mathbf{S}$ cannot be obtained directly from such a vector. To circumvent this problem, we define a binary vector $\mathbf{s}_{\mathrm{b}}$, which is obtained considering the minimum disturbance with respect to $\mathbf{s}_{\mathrm{o}}$ (i.e., $\mathbf{s}_{\mathrm{b}}$ is obtained minimizing its Euclidean distance to $\mathbf{s}_{\mathrm{o}}$). This strategy can be mathematically expressed as follows:

$$\begin{aligned} &\underset{\mathbf{s}_{\mathrm{b}}}{\text{minimize}}\ \|\mathbf{s}_{\mathrm{b}} - \mathbf{s}_{\mathrm{o}}\|^2 \\ &\text{subject to}\ \ [\mathbf{s}_{\mathrm{b}}]_m \in \{0,\ 1\} \\ &\qquad\qquad \mathbf{1}^{\mathrm{T}}\mathbf{s}_{\mathrm{b}} = L. \end{aligned} \tag{28}$$

By rewriting the cost function in (28) as $\|\mathbf{s}_{\mathrm{o}}\|^2 + \|\mathbf{s}_{\mathrm{b}}\|^2 - 2\mathbf{s}_{\mathrm{b}}^{\mathrm{T}}\mathbf{s}_{\mathrm{o}}$ and having the constraints imposing $\|\mathbf{s}_{\mathrm{b}}\|^2 = L$, one can verify that the minimum is attained when the inner product $\mathbf{s}_{\mathrm{b}}^{\mathrm{T}}\mathbf{s}_{\mathrm{o}}$ is maximized. Such a maximization, in turn, can be reached by setting to one the L components of the binary vector $\mathbf{s}_{\mathrm{b}}$ corresponding to the L largest components of $\mathbf{s}_{\mathrm{o}}$. The antenna selection matrix is then determined by making the diagonal of $\mathbf{S}$ equal to $\mathbf{s}_{\mathrm{b}}$ [i.e., $\mathbf{S} = \mathrm{diag}(\mathbf{s}_{\mathrm{b}})$], which is a feasible solution to the original problem (19). It is important to point out that the matrix $\mathbf{S}$ obtained from $\mathbf{s}_{\mathrm{b}}$ will not usually be an optimal solution for (20). Despite this fact, the use of the minimum disturbance as criterion for obtaining $\mathbf{s}_{\mathrm{b}}$ ensures that such a vector will generally be a solution close to the optimal one.

Similarly to (15), the closed-form solution given in (27) requires the *a priori* knowledge of $\mathbf{R}_{\mathrm{x}}$ and $\mathbf{p}$, as well as the inversion of $\mathbf{R}_{\mathrm{rw}}$. Thus, we use the steepest descent method to iteratively obtain $\mathbf{s}$ as follows:

$$\begin{aligned}\mathbf{s}(n+1) &= \mathbf{s}(n) - \mu_{\mathrm{s}}\nabla_{\mathbf{s}}\mathcal{L}(\mathbf{s},\lambda)\\ &= \mathbf{s}(n) - 2\mu_{\mathrm{s}}\mathbf{R}_{\mathrm{rw}}\mathbf{s} + 2\mu\mathbf{r}_{\mathrm{p}} - \mu\lambda\mathbf{1}. \end{aligned} \quad (29)$$

where μ_{s} is the step-size parameter. The Lagrangian multiplier λ can be found in (29) by reinforcing the *a posteriori* constraint $\mathbf{1}^{\mathrm{T}}\mathbf{s}(n+1) = L$, i.e.,

$$\mathbf{1}^{\mathrm{T}}\mathbf{s}(n) - 2\mu\mathbf{1}^{\mathrm{T}}\mathbf{R}_{\mathrm{rw}}\mathbf{s}(n) + 2\mu\mathbf{1}^{\mathrm{T}}\mathbf{r}_{\mathrm{p}} - \mu\lambda\mathbf{1}^{\mathrm{T}}\mathbf{1} = L, \quad (30)$$

which, along with $\mathbf{1}^{\mathrm{T}}\mathbf{1} = M$, leads to

$$\lambda = \frac{\mathbf{1}^{\mathrm{T}}\mathbf{s}(n) - 2\mu\mathbf{1}^{\mathrm{T}}\mathbf{R}_{\mathrm{rw}}\mathbf{s}(n) + 2\mu\mathbf{1}^{\mathrm{T}}\mathbf{r}_{\mathrm{p}} - L}{\mu M}. \quad (31)$$

Then, substituting (31) into (29), we obtain

$$\mathbf{s}(n+1) = \mathbf{P}_{\mathrm{s}}\left[(\mathbf{I} - 2\mu\mathbf{R}_{\mathrm{rw}})\,\mathbf{s}(n) + 2\mu\mathbf{r}_{\mathrm{p}}\right] + \mathbf{f}_{\mathrm{s}} \quad (32)$$

with

$$\mathbf{P}_{\mathrm{s}} = \left[\mathbf{I}_M - \frac{\mathbf{1}\mathbf{1}^{\mathrm{T}}}{M}\right] \quad (33)$$

and

$$\mathbf{f}_{\mathrm{s}} = \frac{L}{M}\mathbf{1}. \quad (34)$$

Finally, using the instantaneous estimates of $\mathbf{R}_{\mathrm{rw}}$ and $\mathbf{r}_{\mathrm{p}}$ given, respectively, by $\mathrm{Re}\left[\mathbf{W}^{\mathrm{H}}(n)\mathbf{x}_{\mathrm{s}}(n)\mathbf{x}_{\mathrm{s}}^{\mathrm{H}}(n)\mathbf{W}(n)\right]$ and $\mathrm{Re}\left[\mathbf{W}^{\mathrm{H}}(n)\mathbf{x}_{\mathrm{s}}(n)\beta_0^*(n)\right]$, we obtain (35), as shown at the bottom of this page.

C. MMSE-BASED AJASB ALGORITHM

The proposed MMSE-based AJASB (MMSE-AJASB) algorithm is based on an iterative scheme that concurrently uses the MMSE-based beamforming strategy from Section III-A and the MMSE-based antenna-selection strategy from Section III-B. Such an algorithm is summarized in Table 1.

From this table, one can notice that, in the first steps, the received signal $\mathbf{x}_{\mathrm{s}}(n)$ is used for computing the beamforming output $y(n)$ and the error signal $e(n)$. Next, the beamforming vector $\mathbf{w}(n)$ is updated by means of the NLMS algorithm presented in Section III-A. Once the *a posteriori* beamforming vector $\mathbf{w}(n+1)$ is calculated, it is further used to compute $\mathbf{s}(n+1)$ considering the algorithm proposed in Section III-B. Finally, the antenna-selection matrix is evaluated by selecting the antennas corresponding to the L largest components of $\mathbf{s}(n+1)$ {such an operation is denoted by *select* $[\mathbf{s}(n+1)]$ in Table 1}.

With respect to computational complexity, in terms of real operations per iteration, the MMSE-based AJASB algorithm requires $17L + M$ sums, $18L + 5$ multiplications, and one division for the beamforming and antenna-selection-vector updates, whereas the remaining *select* operation requires at most $(M - L)L$ real comparisons. In contrast, the standard MMSE-based NLMS beamforming requires $10M$ sums, $10M + 2$ multiplications, and one division. Since in general $M \gg L$, the proposed MMSE-based AJASB algorithm usually has lower computational costs than its NLMS counterpart. The cost of the proposed algorithm is also much smaller than those of the algorithms based on convex optimization solvers, for which the complexity is on the $\mathcal{O}(M^3)$ order.

TABLE 1. Summary of the MMSE-AJASB Algorithm.

Initialize:

$\mu_{\mathrm{w}},\ \mu_{\mathrm{s}},\ \varepsilon$

$\mathbf{P}_{\mathrm{s}} = \left[\mathbf{I}_M - \frac{\mathbf{1}\mathbf{1}^{\mathrm{T}}}{M}\right]$

$\mathbf{w}(0) = [1\ \ 0\ \ \cdots\ \ 0]^T$

$\mathbf{s}(0) = \frac{L}{M}\mathbf{1}$

$\mathbf{S}(0) = \begin{bmatrix} \mathbf{I}_L & \mathbf{0}_{L\times(M-L)} \\ \mathbf{0}_{(M-L)\times L} & \mathbf{0}_{(M-L)\times(M-L)} \end{bmatrix}$

For $n = 0, 1, 2, 3\ldots$

$y(n) = \mathbf{w}^{\mathrm{H}}(n)\mathbf{x}_{\mathrm{s}}(n)$

$e(n) = d(n) - y(n)$

$\mathbf{w}(n) = \mathbf{w}(n) + \mu_{\mathrm{w}}\dfrac{e^*(n)\mathbf{x}_{\mathrm{s}}(n)}{\mathbf{x}_{\mathrm{s}}(n)^{\mathrm{H}}\mathbf{x}_{\mathrm{s}}(n) + \varepsilon}$

$\mathbf{W}(n) = \mathrm{diag}\,[\mathbf{w}(n+1)]$

$\mathbf{s}(n+1) = \mathbf{P}_{\mathrm{s}}\left[\mathbf{I}_M - 2\mu_{\mathrm{s}}\mathrm{Re}\{\mathbf{W}^{\mathrm{H}}(n)\mathbf{x}_{\mathrm{s}}(n)\mathbf{x}_{\mathrm{s}}^{\mathrm{H}}(n)\mathbf{W}(n)\}\right]\mathbf{s}(n) + 2\mu\mathbf{P}_{\mathrm{s}}\mathrm{Re}\{\mathbf{W}^{\mathrm{H}}\mathbf{x}_{\mathrm{s}}(n)d^*(n)\} + \frac{L}{M}\mathbf{1}$

$\mathbf{S}(n+1) = \mathit{select}\,[\mathbf{s}(n+1)]$

Regarding the convergence of the proposed algorithm, an accurate analysis can only be achieved by the corresponding stochastic modeling. However, this type of modeling is very difficult in the case of the proposed algorithm, due to the coupling between the antenna selection matrix and beamforming coefficients. Despite this, it is important to highlight that both the MMSE-based beamforming problem given in (14) and the relaxed antenna selection problem from (20) are convex and their individual adaptive solutions have guaranteed convergence for small values of the step-size parameters [34], even in non-stationary scenarios. As a consequence, the convergence of the concurrent update involved in the proposed method is secured for small values of step size.

IV. MVDR-BASED JOINT ADAPTIVE ANTENNA SELECTION AND BEAMFORMING

In this section, we propose a second alternating-optimization-based adaptive algorithm for solving the JASB problem described in (13). Such an algorithm is formu-

$$\mathbf{s}(n+1) = \mathbf{P}_{\mathrm{s}}\left[\left(\mathbf{I}_M - 2\mu\mathrm{Re}\{\mathbf{W}^{\mathrm{H}}(n)\mathbf{x}_{\mathrm{s}}(n)\mathbf{x}_{\mathrm{s}}^{\mathrm{H}}(n)\mathbf{W}(n)\}\right)\mathbf{s}(n) + 2\mu\mathrm{Re}\{\mathbf{W}^{\mathrm{H}}(n)\mathbf{x}_{\mathrm{s}}(n)d^*(n)\}\right] + \mathbf{f}_{\mathrm{s}}. \quad (35)$$

lated considering the MVDR criterion, which allows for $\Phi(\mathbf{w}, \mathbf{S}) = \mathrm{E}\left[|y(n)|^2\right]$ along with an additional constraint to ensure unit gain towards the SOI direction.

A. MVDR BEAMFORMING

In the context of beamforming optimization, the linearly constrained minimum variance (LCMV) criterion has been widely used specially due to its convexity property [39]. Such a criterion is focused on minimizing the variance of the beamformer output $y(n)$ subject to a set of linear constraints. Particularly, using a single linear constraint that ensures unit gain towards the SOI direction, the criterion is known as the MVDR problem, which leads to the SINR maximization [1].

For the scenario considered here, the MVDR beamforming problem is formulated as follows:

$$\begin{aligned} &\underset{\mathbf{w}}{\text{minimize}}\ \mathbf{w}^{\mathrm{H}}\mathbf{S}\mathbf{R}_{\mathrm{x}}\mathbf{S}\mathbf{w} \\ &\text{subject to}\ \mathbf{w}^{\mathrm{H}}\mathbf{S}\mathbf{a}(\theta_0) = 1. \end{aligned} \tag{36}$$

It is important to notice that, if all antennas are selected (i.e., $\mathbf{S} = \mathbf{I}_M$), (36) becomes the original MVDR problem.

The closed-form solution for (36), given by

$$\mathbf{w}_{\mathrm{o}} = \frac{(\mathbf{S}\mathbf{R}_{\mathbf{x}}\mathbf{S})^{\dagger}\mathbf{S}\mathbf{a}(\theta_0)}{\mathbf{a}(\theta_0)^{\mathrm{H}}\mathbf{S}(\mathbf{S}\mathbf{R}_{\mathbf{x}}\mathbf{S})^{\dagger}\mathbf{S}\mathbf{a}(\theta_0)} \tag{37}$$

requires knowledge of $\mathbf{R}_{\mathrm{x}}$ (which is usually not available) and the computation of $(\mathbf{S}\mathbf{R}_{\mathbf{x}}\mathbf{S})^{\dagger}$ (computationally costly). To circumvent these problems, we adopt the same reasoning used for developing the CLMS algorithm [30]. Thus, the following beamforming update equation is obtained:

$$\mathbf{w}(n+1) = \mathbf{P}_{\mathrm{a}}(n)\left[\mathbf{w}(n) - \mu_{\mathrm{w}}\, y^*(n)\mathbf{x}_{\mathrm{s}}(n)\right] + \mathbf{f}_{\mathrm{a}}(n) \tag{38}$$

where μ_{w} is the step size,

$$\mathbf{P}_{\mathrm{a}}(n) = \left[\mathbf{I}_M - \frac{\mathbf{S}(n)\mathbf{a}(\theta_0)\mathbf{a}^{\mathrm{H}}(\theta_0)\mathbf{S}(n)}{\mathbf{a}^{\mathrm{H}}(\theta_0)\mathbf{S}(n)\mathbf{a}(\theta_0)}\right] \tag{39}$$

and

$$\mathbf{f}_{\mathrm{a}}(n) = \frac{\mathbf{S}(n)\mathbf{a}(\theta_0)}{\mathbf{a}^{\mathrm{H}}(\theta_0)\mathbf{S}(n)\mathbf{a}(\theta_0)}. \tag{40}$$

The normalized version of the CLMS [30], termed constrained CNLMS algorithm, provides faster convergence and lower misadjustment as compared with the original CLMS. Thus, taking into account such performance improvements, we obtain the CNLMS algorithm by dividing μ_{w} by $\mathbf{x}_{\mathrm{s}}^{\mathrm{H}}(n)\mathbf{P}_{\mathrm{a}}(n)\mathbf{x}_{\mathrm{s}}(n)$ in (38). Thereby,

$$\mathbf{w}(n+1) = \mathbf{P}_{\mathrm{a}}(n)\left[\mathbf{w}(n) - \frac{\mu_{\mathrm{w}}\, y^*(n)\mathbf{x}_{\mathrm{s}}(n)}{\mathbf{x}_{\mathrm{s}}^{\mathrm{H}}(n)\mathbf{P}_{\mathrm{a}}(n)\mathbf{x}_{\mathrm{s}}(n)}\right] + \mathbf{f}_{\mathrm{a}}(n). \tag{41}$$

B. MVDR ANTENNA SELECTION

The proposed MVDR antenna selection method is based on finding the antenna subset that minimizes the variance of the beamforming output signal, without suppressing the gain towards the SOI direction. More specifically, such a method is derived from the following optimization problem:

$$\begin{aligned} &\underset{\mathbf{S}}{\text{minimize}}\ \mathbf{w}^{\mathrm{H}}\mathbf{S}\mathbf{R}_{\mathrm{x}}\mathbf{S}\mathbf{w} \\ &\text{subject to}\ [\mathbf{S}]_{m,m} \in \{0,\ 1\} \\ &\qquad\qquad \mathrm{Tr}\,(\mathbf{S}) = L \\ &\qquad\qquad \mathrm{Re}\{\mathbf{w}^{\mathrm{H}}\mathbf{S}\mathbf{a}(\theta_0)\} = 1. \end{aligned} \tag{42}$$

Note that only the real part of $\mathbf{w}^{\mathrm{H}}\mathbf{S}\mathbf{a}(\theta_0)$ is constrained in (42), resulting in a loosen constraint as compared with the corresponding one in (36). This procedure can be done since such a constraint is sufficient to prevent $\mathbf{S}$ from suppressing the SOI and the unit gain in the SOI direction is enforced by the beamforming update.

Similarly to (19), the MVDR antenna selection problem in (42) is also an NP-hard problem due to the binary constraints. Therefore, we again relax these constraints by allowing $[\mathbf{S}]_{m,m}$ to be a real number. Then, considering the auxiliary vector $\mathbf{s}$ (diagonal vector of $\mathbf{S}$) and matrix $\mathbf{W} = \mathrm{diag}(\mathbf{w})$, the resulting optimization problem becomes

$$\begin{aligned} &\underset{\mathbf{s}\in\mathbb{R}^M}{\text{minimize}}\ \mathbf{s}^{\mathrm{T}}\mathbf{W}^{\mathrm{H}}\mathbf{R}_{\mathrm{x}}\mathbf{W}\mathbf{s} \\ &\text{subject to}\ \mathbf{1}^{\mathrm{T}}\mathbf{s} = L \\ &\qquad\qquad \mathrm{Re}\{\mathbf{s}^{\mathrm{T}}\mathbf{W}^{\mathrm{H}}\mathbf{S}\mathbf{a}(\theta_0)\} = 1. \end{aligned} \tag{43}$$

Note that the last constraint in (43) is derived from the last constraint in (42) by considering the idempotent property of $\mathbf{S}$. In fact, matrix $\mathbf{S}$ is not treated as an optimization variable in (43) and is used for ensuring unit gain for the SOI considering the *a priori* antenna selection.

In order to find the optimal solution for (43), we first obtain the corresponding Lagrangian function as

$$\mathcal{L}(\mathbf{s}, \lambda, \alpha) = \mathbf{s}^{\mathrm{T}}\mathbf{R}_{\mathrm{rw}}\mathbf{s} + \lambda(\mathbf{1}^{\mathrm{T}}\mathbf{s} - L) + \alpha\left(\mathbf{s}^{\mathrm{T}}\mathbf{r}_{\mathrm{a}} - 1\right) \tag{44}$$

where λ and α are Lagrange multipliers,

$$\mathbf{R}_{\mathrm{rw}} = \mathrm{Re}\{\mathbf{W}^{\mathrm{H}}\mathbf{R}_{\mathbf{x}}\mathbf{W}\} \tag{45}$$

and

$$\mathbf{r}_{\mathrm{a}} = \mathrm{Re}\{\mathbf{W}^{\mathrm{H}}\mathbf{S}\mathbf{a}(\theta_0)\}. \tag{46}$$

Next, taking the gradient of (44) with respect to $\mathbf{s}$, one has

$$\nabla_{\mathbf{s}}\mathcal{L}(\mathbf{s}, \lambda, \alpha) = 2\mathbf{R}_{\mathrm{rw}}\mathbf{s} + \lambda\mathbf{1} + \alpha\mathbf{r}_{\mathrm{a}} \tag{47}$$

and setting it equal to zero, we can obtain

$$\mathbf{s}_{\mathrm{o}} = -\frac{1}{2}\mathbf{R}_{\mathrm{rw}}^{-1}\left(\lambda\mathbf{1} + \alpha\mathbf{r}_{\mathrm{a}}\right). \tag{48}$$

Finally, applying the constraints of (43) in (48) to obtain λ and α, and substituting them back into (48), we have

$$\begin{aligned} \mathbf{s}_{\mathrm{o}} = &\left[\frac{\mathbf{R}_{\mathrm{rw}}^{-1}}{\mathbf{1}^{\mathrm{T}}\mathbf{R}_{\mathrm{rw}}^{-1}\mathbf{1}\mathbf{r}_{\mathrm{a}}^{\mathrm{T}}\mathbf{R}_{\mathrm{rw}}^{-1}\mathbf{r}_{\mathrm{a}} - \mathbf{1}^{\mathrm{T}}\mathbf{R}_{\mathrm{rw}}^{-1}\mathbf{r}_{\mathrm{a}}\mathbf{r}_{\mathrm{a}}^{\mathrm{T}}\mathbf{R}_{\mathrm{rw}}^{-1}\mathbf{1}}\right] \\ &\times\left[(L\cdot\mathbf{r}_{\mathrm{a}}^{\mathrm{T}}\mathbf{R}_{\mathrm{rw}}^{-1}\mathbf{r}_{\mathrm{a}} - \mathbf{1}^{\mathrm{T}}\mathbf{R}_{\mathrm{rw}}^{-1}\mathbf{r}_{\mathrm{a}})\mathbf{1}\right. \\ &\left.+(\mathbf{1}^{\mathrm{T}}\mathbf{R}_{\mathrm{rw}}^{-1}\mathbf{1} - L\cdot\mathbf{r}_{\mathrm{a}}^{\mathrm{T}}\mathbf{R}_{\mathrm{rw}}^{-1}\mathbf{1})\mathbf{r}_{\mathrm{a}}\right]. \end{aligned} \tag{49}$$

Similarly to our discussion in Section III-B, the optimal solution given in (49) cannot be directly used for obtaining the *a posteriori* selection matrix. In this case, considering the minimum disturbance criteria considered in (28), the antenna selection is performed by setting the diagonal elements of $\mathbf{S}$ corresponding to the L highest values of $\mathbf{s}_o$ to one, while the remaining $M - L$ diagonal elements are set to zero. Moreover, the evaluation of the closed-form solution in (49) requires knowledge of $\mathbf{R}_x$ and demands the computation of $\mathbf{R}_{rw}$. Therefore, we propose an adaptive procedure based on the CLMS algorithm [30] for obtaining $\mathbf{s}_o$. Such a procedure is derived by applying the steepest-descent method to (43), which results in

$$\mathbf{s}(n+1) = \mathbf{s}(n) - \mu_s \nabla_{\mathbf{s}} \mathcal{L}(\mathbf{s}, \lambda, \alpha) \tag{50}$$

where μ_s is the step size. Then, substituting (47) into (50), we obtain

$$\mathbf{s}(n+1) = [\mathbf{I}_M - 2\mu_s \mathbf{R}_{rw}]\,\mathbf{s}(n) - \mu_s \lambda \mathbf{1} - \mu_s \alpha \mathbf{r}_a. \tag{51}$$

Regarding λ and α, their corresponding values are found by reinforcing the constraints of (43) with $\mathbf{s}(n+1)$, i.e., by solving the following linear system:

$$\begin{cases} \mathbf{1}^T \mathbf{s}(n+1) = L \\ \mathbf{s}^T(n+1)\mathbf{r}_a = 1. \end{cases} \tag{52}$$

The solution of (52) leads to

$$\lambda = \frac{\left[\mathbf{s}^T(n) - 2\mu_s \mathbf{s}^T(n)\mathbf{R}_{rw}\right]\left(\|\mathbf{r}_a\|^2 \mathbf{1} - \mathbf{r}_a\right) - L\|\mathbf{r}_a\|^2 + 1}{\mu_s\left(\|\mathbf{r}_a\|^2 M - 1\right)} \tag{53}$$

and

$$\alpha = \frac{\left[\mathbf{s}^T(n) - 2\mu_s \mathbf{s}^T(n)\mathbf{R}_{rw}\right](M\mathbf{r}_a - \mathbf{1}) + L - M}{\mu_s\left(\|\mathbf{r}_a\|^2 M - 1\right)} \tag{54}$$

which are substituted into (51) to obtain

$$\mathbf{s}(n+1) = \mathbf{P}_g\,[\mathbf{I}_M - 2\mu_s \mathbf{R}_{rw}]\,\mathbf{s}(n) + \mathbf{f}_g \tag{55}$$

with

$$\mathbf{P}_g = \mathbf{I}_M - \frac{\|\mathbf{r}_a\|^2 \mathbf{1}\mathbf{1}^T - \mathbf{1}\mathbf{r}_a^T - \mathbf{r}_a\mathbf{1}^T + M\mathbf{r}_a\mathbf{r}_a^T}{\|\mathbf{r}_a\|^2 M - 1} \tag{56}$$

and

$$\mathbf{f}_g = \frac{\left(L\|\mathbf{r}_a\|^2 - 1\right)\mathbf{1} + (M-L)\,\mathbf{r}_a}{\|\mathbf{r}_a\|^2 M - 1}. \tag{57}$$

Finally, we can further evaluate (55) using the instantaneous estimates of $\mathbf{R}_{rw}$ and $\mathbf{r}_a$, which are given by $\mathrm{Re}\{\mathbf{W}^H(n)\mathbf{x}_s(n)\mathbf{x}_s^H(n)\mathbf{W}(n)\}$ and $\mathrm{Re}\{\mathbf{W}^H(n)\mathbf{S}(n)\mathbf{a}(\theta_0)\}$, respectively.

TABLE 2. Summary of the MVDR-AJASB Algorithm.

Initialize:

$\mu_w,\ \mu_s,\ \varepsilon$

$\mathbf{P}_s = \left[\mathbf{I}_M - \frac{\mathbf{1}\mathbf{1}^T}{M}\right]$

$\mathbf{w}(0) = [1\ \ 0\ \ \cdots\ \ 0]^T$

$\mathbf{s}(0) = \frac{L}{M}\mathbf{1}$

$\mathbf{S}(0) = \begin{bmatrix} \mathbf{I}_L & \mathbf{0}_{L\times(M-L)} \\ \mathbf{0}_{(M-L)\times L} & \mathbf{0}_{(M-L)\times(M-L)} \end{bmatrix}$

For $n = 0, 1, 2, 3 \ldots$

$y(n) = \mathbf{w}^H(n)\mathbf{x}_s(n)$

$\mathbf{P}_a(n) = \left[\mathbf{I}_M - \frac{\mathbf{S}(n)\mathbf{a}(\theta_0)\mathbf{a}^H(\theta_0)\mathbf{S}(n)}{\mathbf{a}^H(\theta_0)\mathbf{S}(n)\mathbf{a}(\theta_0)}\right]$

$\mathbf{f}_a(n) = \frac{\mathbf{S}(n)\mathbf{a}(\theta_0)}{\mathbf{a}^H(\theta_0)\mathbf{S}(n)\mathbf{a}(\theta_0)}$

$\mathbf{w}(n+1) = \mathbf{P}_a(n)\left[\mathbf{w}(n) - \frac{\mu_w\, y^*(n)\mathbf{x}_s(n)}{\mathbf{x}_s^H(n)\mathbf{P}_a(n)\mathbf{x}_s(n) + \varepsilon}\right] + \mathbf{f}_a(n)$

$\mathbf{W}(n) = \mathrm{diag}\,[\mathbf{w}(n+1)]$

$\mathbf{R}_{rw} = \mathrm{Re}\{\mathbf{W}^H(n)\mathbf{x}_s(n)\mathbf{x}_s^H(n)\mathbf{W}(n)\}$

$\mathbf{r}_a = \mathrm{Re}\{\mathbf{W}^H(n)\mathbf{S}(n)\mathbf{a}(\theta_0)\},$

$\mathbf{P}_g = \mathbf{I}_M - \frac{\|\mathbf{r}_a\|^2\mathbf{1}\mathbf{1}^T - \mathbf{1}\mathbf{r}_a^T - \mathbf{r}_a\mathbf{1}^T + M\mathbf{r}_a\mathbf{r}_a^T}{\|\mathbf{r}_a\|^2 M - 1}$

$\mathbf{f}_g = \frac{\left(L\|\mathbf{r}_a\|^2 - 1\right)\mathbf{1}_M + (M-L)\,\mathbf{r}_a}{\|\mathbf{r}_a\|^2 M - 1}$

$\mathbf{s}(n+1) = \mathbf{P}_g\,[\mathbf{I}_M - 2\mu_s\mathbf{R}_{rw}]\,\mathbf{s}(n) + \mathbf{f}_g$

$\mathbf{S}(n+1) = \mathit{select}\,[\mathbf{s}(n+1)]$

C. MVDR-BASED AJASB ALGORITHM

The proposed MVDR-based AJASB (MVDR-AJASB) algorithm consists of an iterative process that concurrently uses the beamforming strategy described in Section IV-A and the antenna selection strategy from Section IV-B. Such an algorithm is summarized in Table 2.

From Table 2, one can notice that, in the first step, the received signal $\mathbf{x}_s(n)$ is used for computing the beamforming output $y(n)$. Next, the beamforming vector $\mathbf{w}(n)$ is updated by means of the CNLMS-based algorithm presented in Section IV-A. Once the *a posteriori* beamforming vector $\mathbf{w}(n+1)$ is calculated, it is further used to compute $\mathbf{s}(n+1)$ considering the algorithm proposed in Section IV-B. Finally, the antenna-selection matrix is evaluated by selecting the antennas corresponding to the L largest components of $\mathbf{s}(n+1)$, denoted in Table 2 by $\mathit{select}\,[\mathbf{s}(n+1)]$. A regularization parameter ε has also been included in the update equations of $\mathbf{w}(n)$ to prevent divisions by very small values.

Regarding the computational burden, the MVDR-based AJASB requires $3M + 36L - 4$ sums, $M + 39L + 18$ multiplications, and three divisions, plus at most $(M-L)L$ real comparisons for the *select* operation. In contrast, the MVDR-based CNLMS beamforming requires $24M-4$ sums, $24M+8$ multiplications, and two divisions. As $M \gg L$, the proposed MVDR-based AJASB also has lower computational complexity, as compared with its CNLMS counterpart.

Similarly to the MMSE-AJASB algorithm presented in Section III, the stochastic modeling required for an accurate

convergence analysis is very hard to be carried out due to the coupling between the antenna selection matrix and beamforming vector. However, both CLMS and CNLMS algorithms considered in the proposed approach have guaranteed convergence when the step-size parameters are small [34]. Thereby, the convergence of the MVDR-AJASB algorithm is also ensured for small values of step size.

V. SIMULATION RESULTS

In this section, we present simulation results that aim at assessing the performance of the proposed algorithms and make comparisons with other beamforming algorithms from the literature. In this context, the performance of the proposed MMSE-AJASB algorithm (see Section III) is compared with that of the MMSE-based NLMS beamforming algorithm. Two versions of the NLMS beamforming algorithms are in fact considered in our simulations; the first using all M antennas of the subarray (denoted NLMS-M) and the second using only the first L antennas (termed NLMS-L). On the other hand, the performance of the proposed MVDR-AJASB algorithm (see Section IV) is compared with that of the MVDR-based CNLMS beamforming algorithm without the use of antenna selection. Again, two versions of the CNLMS beamforming algorithm are considered; one using all M antennas (CNLMS-M) and other using only the first L antennas. It is important to highlight that the antenna-selection algorithms based on convex optimization solvers available in the open literature are not considered in our comparisons, since they do not provide real-time processing, which is the focus in this research work. Moreover, as mentioned at the Introduction (Section I), other AJASB algorithms from the literature do not abide by the limited number of RF chains, and thus, they cannot be fairly compared with the proposed algorithms.

Four different experiments are presented in this section, all considering a uniform linear array with half-wavelength spacing between consecutive elements, which results in a steering vector given by

$$\mathbf{a}(\theta_i) = [1 \;\; \mathrm{e}^{-j\pi \sin\theta_i} \;\; \mathrm{e}^{-j2\pi \sin\theta_i} \;\; \cdots \;\; \mathrm{e}^{-j(M-1)\pi \sin\theta_i}]^{\mathrm{T}}. \quad (58)$$

This type of array is chosen without loss of generality, since the proposed algorithms can also be effectively applied to other array geometries, such as planar, circular, or non-uniform. In all experiments, the algorithms have their beamforming vectors initialized with $\mathbf{w}(0) = [1 \;\; 0 \;\; \cdots \;\; 0]^{\mathrm{T}}$, which corresponds to an omnidirectional radiation pattern over the azimuth plane. The auxiliary antenna-selection vector is initialized as $\mathbf{s}(0) = (L/M)\mathbf{1}$ and the antenna-selection matrix $\mathbf{S}$ is initialized in such a way that the L leftmost antenna elements are selected. The symbols are generated from a zero-mean unit-variance Gaussian distribution and the normalized power (relative to the noise variance) of the transmitted signals is of 30 dB. Since the interfering signals come from co-channel cells, they are attenuated by 20 dB due to free-space path loss.

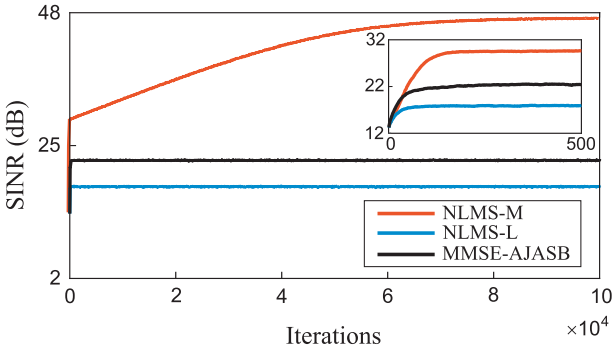

FIGURE 2. Example 1. SINR curves of the MMSE-based algorithms for $M = 64$ and $L = 4$.

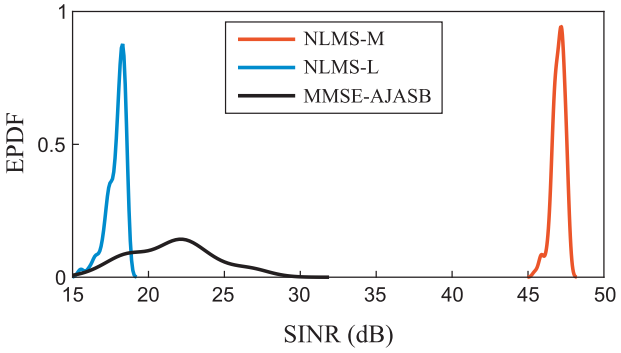

FIGURE 3. Example 1. EPDF curves for the MMSE-based algorithms with $M = 64$ and $L = 4$.

The performance of the algorithms is assessed in terms of transient SINR, and/or empirical probability density function (EPDF) of the steady-state SINR, all obtained in the context of Monte Carlo simulations with 200 independent runs. The steady-state values used for obtaining the EPDF curves are those from the end of each individual Monte Carlo run.

A. EXPERIMENT 1

In this first experiment, a stationary scenario is considered where the subarray allocated to a given intra-cell user (SOI) is equipped with $M = 64$ antennas and initially with $L = 4$ RF chains. We further assume $K = 6$ inter-cell users, with the SOI positioned at 0°, and five interferers located at −35°, −10°, 12°, 25°, and 40°. The step-size parameters were adjusted to provide similar initial convergence rates, resulting in the following values: $\mu = 1$ for both the NLMS-M and NLMS-L; $\mu = 0.002$ for both the CNLMS-M and CNLMS-L; $\mu_{\mathrm{w}} = 1$ and $\mu_{\mathrm{s}} = 0.01$ for the MMSE-AJASB; $\mu_{\mathrm{w}} = 0.002$ and $\mu_{\mathrm{s}} = 0.001$ for the MVDR-AJASB.

For the MMSE-based algorithms, the obtained SINR curves are shown in Fig. 2, whereas the EPDF curves are depicted in Fig. 3. From these figures, one can notice that the proposed algorithm outperforms the NLMS-L by more than 4.5 dB in terms of average steady-state SINR performance (see Fig. 2), achieving also higher steady-state SINR values in most of the experimental runs (see Fig. 3). In fact, the best run of the proposed algorithm provided an SINR

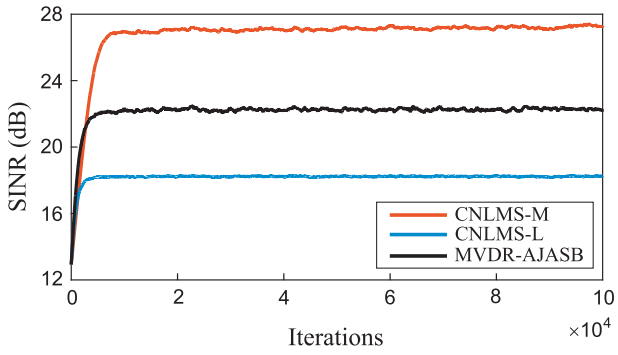

FIGURE 4. Example 1. SINR curves of the MVDR-based algorithms for $M = 64$ and $L = 4$.

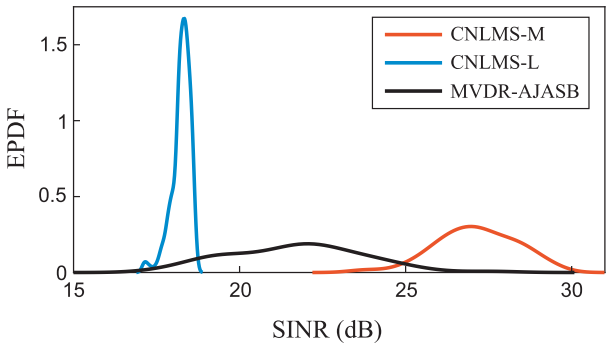

FIGURE 5. Example 1. EPDF curves for the MVDR-based algorithms with $M = 64$ and $L = 4$.

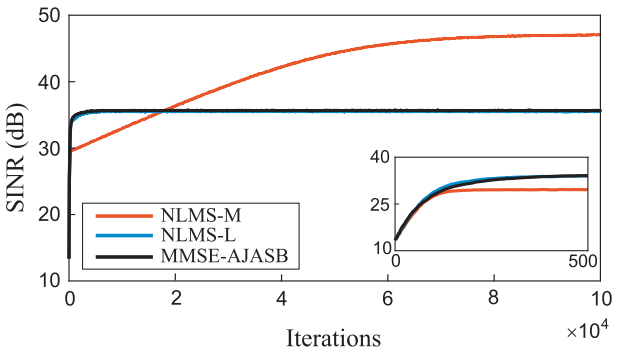

FIGURE 6. Example 1. SINR curves of the MMSE-based algorithms for $M = 64$ and $L = 8$.

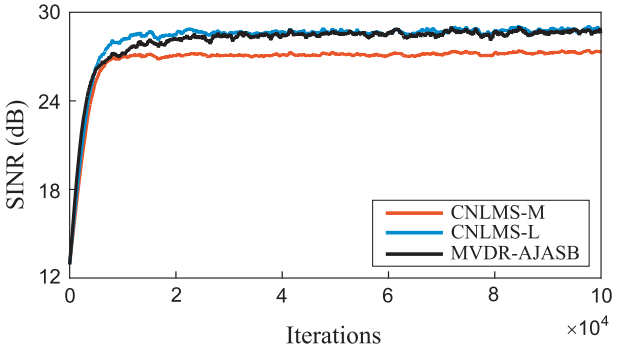

FIGURE 7. Example 1. SINR curves of the MVDR-based algorithms for $M = 64$ and $L = 8$.

that is more than 10 dB higher than that of the best run of the NLMS-L. The NLMS-M algorithm obtained the best steady-state performance, which is an expected result in the considered scenario since the number of RF chains used by this algorithm is 16 times larger than that of the others (64 RF chains versus 4 for both the NLMS-L and proposed one).

The results obtained by the MVDR-based algorithms are shown in Figs. 4 and 5. From these figures, we verify that the proposed algorithm outperforms the CNLMS-L by nearly 4 dB in terms of average steady-state SINR. Moreover, the proposed algorithm outperforms the CNLMS-L in most of the runs and provides steady-state SINR levels higher than 25 dB in some runs. As expected, the CNLMS-M presents a better performance in comparison with the other algorithms (due to the significantly larger number of RF chains used).

Also in the context of this first experiment, the number of RF chains is changed from $L = 4$ to $L = 8$. This case is of particular interest since it consists of a fairly favorable scenario in which the SOI is positioned afar from the interfering signals and the number of RF chains is larger than the number of users. The SINR curves obtained for the MMSE-based algorithms (depicted in Fig. 6) show that the proposed algorithm and the NLMS-L have nearly the same performance. This result is expected, since we do not assume different fading among the antennas, and the additional RF chains allow high levels of interference suppression for any combination of antennas. Moreover, in the case of the MVDR-based algorithms, whose results are shown in Fig. 7, the proposed algorithm is capable of attaining a performance similar to that of the CNLMS-M, while operating with 1/8 of RF chains. The difference of these algorithms with respect to the CNLMS-L is small, this is due to the favorable scenario considered in this example.

B. EXPERIMENT 2

In this experiment, we would like to verify the performance of the proposed algorithms in a scenario where the SOI is positioned nearly in the same direction as one of the interferers. We assume that the system is operating with $L = 8$ RF chains and the SOI is located at 11°, while the interferer positions and all other parameters are the same as in Experiment 1. Here, we assess the transient SINR and the radiation pattern obtained at the last iteration of one Monte Carlo run.

The SINR curves obtained for the MMSE-based algorithms are shown in Fig. 8. In comparison with the results from Experiment 1 with $L = 8$ RF chains, the steady-state SINRs obtained here for both the NLMS-M and the proposed algorithm are approximately 3% lower than the corresponding steady-state values from Fig. 6, whereas a reduction of 42% is observed for the NLMS-L. These results demonstrate the robustness of the proposed algorithm to adverse scenarios in comparison with the beamforming algorithms without the use of antenna selection, using the same number of RF chains. The SINR results regarding the MVDR-based algorithms are shown in Fig. 9. In this case, the robustness of the proposed algorithm is even more evident, i.e., while

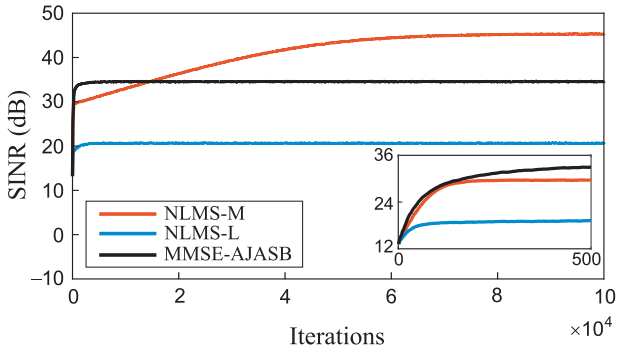

FIGURE 8. Example 2. SINR curves of the MMSE-based algorithms for $M = 64$ and $L = 8$.

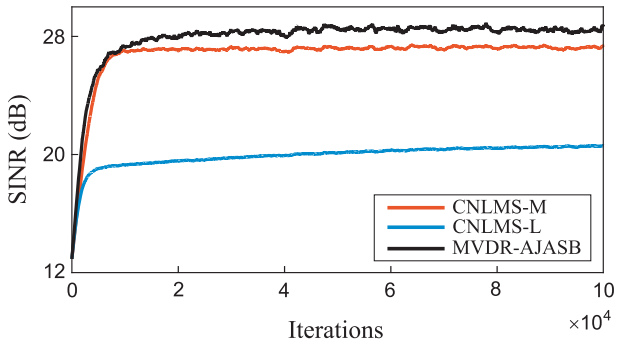

FIGURE 9. Example 2. SINR curves of the MVDR-based algorithms for $M = 64$ and $L = 8$.

the SINR of the CNLMS-L has fallen by nearly 28% in comparison with the previous experiment, the SINR obtained by our algorithm has fallen by less than 0.4%.

The gains at the directions of the SOI and the interferers, obtained from the radiation patterns at the last iteration of a given Monte Carlo run of each algorithm, are summarized in Tables 3 and 4. These results show that, in the case of the MMSE-based algorithms, both the NLMS-M and the proposed MMSE-AJASB algorithms are capable of significantly attenuating the interferer at 12° (the one close to the SOI), attaining attenuations of 10.02 dB and 17.64 dB, respectively, whereas the NLMS-L has attained an attenuation level of only 1.42 dB. Similarly, for the MVDR-based algorithms, the attenuation at this particular direction is nearly 8.8 dB for the CNLMS-M, 6.4 dB for the proposed MVDR-AJASB, and only 1.0 dB for the CNLMS-L. In addition, note that all MVDR-based algorithms attain unit gain (0 dBi) at the SOI direction, as required by the MVDR criterium.

C. EXPERIMENT 3

In this third experiment, we assess the impact of the number of RF chains on the steady-state performance of the proposed algorithms. We assume that the BS is equipped with $M = 64$ antenna elements and assess the steady-state SINR for $L = 4, 8, 16, 32,$ and 64 RF chains. The steady-state SINR is obtained by averaging the SINR values achieved after 2×10^6 iterations of each Monte Carlo run. We further assume $K = 6$ users, with the SOI positioned at 5°, and five

TABLE 3. Gain (in dBi) at the direction of the SOI and the interferers for the MMSE-based algorithms.

θ	NLMS-M	NLMS-L	MMSE-AJASB
11°	-0.01	0.10	0.01
-35°	-37.80	-6.89	-12.87
-10°	-20.02	-6.74	-13.96
12°	-17.64	-1.42	-10.02
25°	-20.86	-5.41	-12.79
40°	-19.27	-6.53	-6.70

TABLE 4. Gain (in dBi) at the direction of the SOI and the interferers for the MMSE-based algorithms.

θ	CNLMS-M	CNLMS-L	MVDR-AJASB
11°	0.00	0.00	0.00
-35°	-7.31	-6.06	-7.40
-10°	-11.01	-8.57	-11.71
12°	-8.78	-1.01	-6.36
25°	-11.96	-6.53	-9.11
40°	-3.88	-4.22	-4.49

interferers located at −42°, −18°, 25°, 44°, and 6° (the last one is very close to the SOI). The step sizes for the considered algorithms are: $\mu = 0.5$ for both the NLMS-M and NLMS-L; $\mu = 0.002$ for both the CNLMS-M and CNLMS-L; $\mu_w = 0.5$ and $\mu_s = 0.01$ for the MMSE-AJASB; $\mu_w = 0.002$ and $\mu_s = 0.001$ for the MVDR-AJASB.

The results obtained for the MMSE-based algorithms are depicted in Fig. 10, while Fig. 11 shows the results obtained for the MVDR-based algorithms. These results show that the array gain provided by the proposed algorithms increases much more as the number of RF chains increases in comparison with the beamforming algorithms without the use of antenna selection. Moreover, it is important to highlight that, except for the cases in which $L < K$, the SINR levels obtained by the proposed algorithms are closer to those obtained by using the complete array (i.e., NLMS-M and CNLMS-M) than to those obtained by the arrays with reduced number of RF chains (NLMS-L and CNLMS-L). In particular, the MVDR-AJASB has nearly the same performance as the CNLMS-M when $L \geq 16$ RF chains, meaning that almost the same performance can be obtained by using a number as low as one fourth of RF chains.

D. EXPERIMENT 4

In this last example, we examine a nonstationary scenario where the SOI is initially positioned at 15° and moves toward 0° between iterations 50,000 and 70,000 at a constant angular speed. The interferers are positioned at −45°, −10°, 5°, 25°, and 40°, while the corresponding subarray has $M = 32$ antennas and $L = 4$ RF chains. Here, the step sizes used are the same as in Experiment 1.

In Figs. 12 and 13, we show the SINR curves for the MMSE- and the MVDR-based algorithms, respectively. In these figures, one can observe a clear advantage of the proposed algorithms over their counterparts that use the same number of RF chains. Moreover, as comparing the

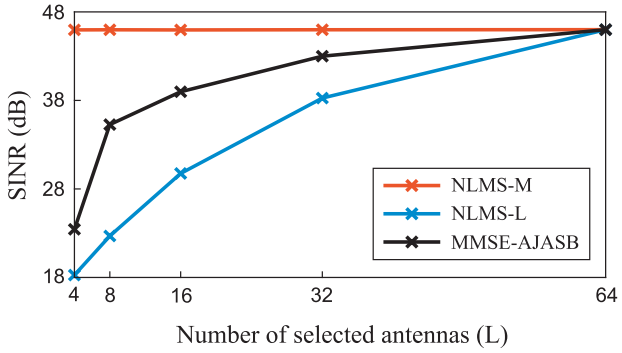

FIGURE 10. Example 3. Steady-state SINR curves for different numbers of RF chains using the MMSE-based algorithms.

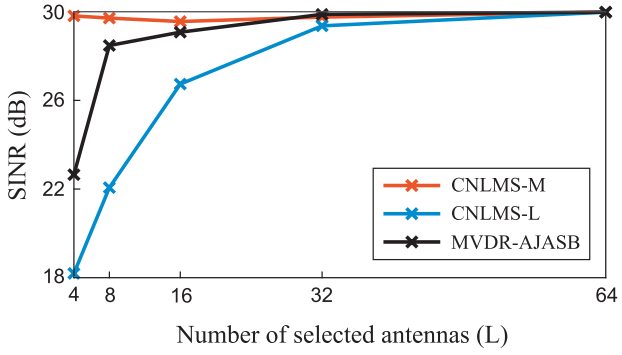

FIGURE 11. Example 3. Steady-state SINR curves for different numbers of RF chains using the MVDR-based algorithms.

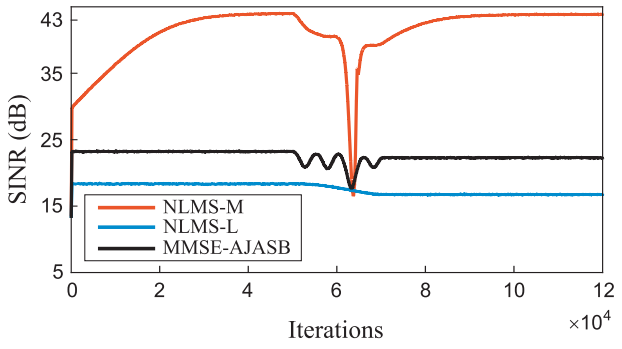

FIGURE 12. Example 4. SINR curves for the MMSE-based algorithms in the nonstationary scenario.

steady-state SINR before iteration 50,000 with that at the end of the process, we note that: i) the SINR obtained for both the NLMS-M and the CNLMS-M have no significant difference; ii) the SINR falls by 8.8% and 8% for the NLMS-L and the CNLMS-L, respectively; and iii) smaller falls of nearly 4.1% and 5.7% are observed, respectively, for the proposed MMSE-AJASB and MVDR-AJASB algorithms. Such results confirm the ability of the proposed algorithms to track the SOI and attenuate the interfering signals in nonstationary scenarios.

E. DISCUSSION

The examples presented in this section show that the proposed MMSE-AJASB and MVDR-AJASB algorithms can achieve high SINR levels with a limited number of RF chains.

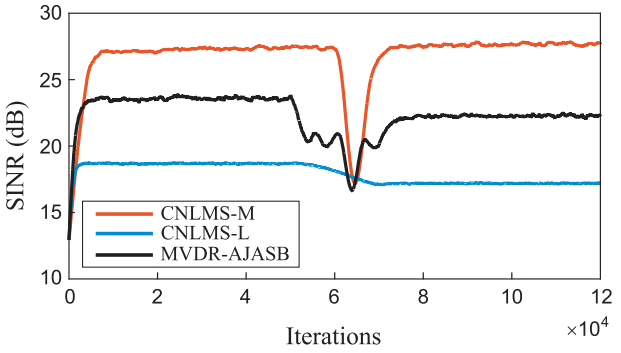

FIGURE 13. Example 4. SINR curves for the MVDR-based algorithms in the nonstationary scenario.

Especially in scenarios with $L \leq K$ or in cases where the SOI is positioned close to the interfering signals, the proposed algorithms can perform almost as well as the algorithms operating with $L = M$. In particular, Experiment 1 shows that the proposed algorithms are able to achieve a very good performance even when the number of RF chains is smaller than the number of interferers. Experiment 2 shows the ability of the proposed algorithms to work in a severe condition, such as when the SOI is close to an interfering signal. Experiment 3 illustrates the impact of the number of available RF chains on the performance of the algorithms. We note that once the number of RF chains is enough to place nulls in the direction of the interfering signals, i.e. $L > K + 1$ [1], the proposed algorithms can provide SINR levels close to those achieved by the NLMS-M and CNLMS-M algorithms. Finally, Experiment 4 confirms the ability of the proposed algorithms to track channel variations, providing high SINR levels in nonstationary environments.

VI. CONCLUDING REMARKS

In this paper, we have proposed two new adaptive algorithms to solve the JASB problem for uplink reception in mobile communication systems. The first algorithm is based on an iterative alternating optimization procedure, in which the beamforming vector and the antenna selection matrix are computed by using the MMSE criterion. Next, a similar alternating optimization procedure based on the MVDR criterion is used to derive the second algorithm. Numerical simulation results showed that the proposed algorithms led to high SINR levels in adverse scenarios, such as those with less RF chains than users, with interfering signals located at the vicinity of the SOI, and nonstationary environments. Thereby, based on the obtained results, we can conclude that the effectiveness of the proposed algorithms have been shown.

REFERENCES

[1] C. A. Balanis and P. I. Ioannides, *Introduction to Smart Antennas*. San Rafael, CA, USA: Morgan & Claypool Publishers, 2007.
[2] J. H. Winters, "Smart antennas for wireless systems," *IEEE Pers. Commun.*, vol. 5, no. 1, pp. 23–27, Feb. 1998.
[3] A. Goldsmith, *Wireless Communications*. New York, NY, USA: Cambridge Univ. Press, 2005.

[4] T. L. Marzetta, "Noncooperative cellular wireless with unlimited numbers of base station antennas," *IEEE Trans. Wireless Commun.*, vol. 9, no. 11, pp. 3590–3600, Nov. 2010.

[5] R. W. Heath, N. González-Prelcic, S. Rangan, W. Roh, and A. M. Sayeed, "An overview of signal processing techniques for millimeter wave MIMO systems," *IEEE J. Sel. Topics Signal Process.*, vol. 10, no. 3, pp. 436–453, Apr. 2016.

[6] A. Ghrayeb, "A survey on antenna selection for MIMO communication systems," in *Proc. 2nd Int. Conf. Inf. Commun. Technol., Theory Appl. (ICTTA)*, Damascus, Syria, Apr. 2006, pp. 2104–2109.

[7] A. F. Molisch and M. Z. Win, "MIMO systems with antenna selection," *IEEE Commun. Mag.*, vol. 5, no. 1, pp. 46–56, Mar. 2004.

[8] X. Gao, O. Edfors, J. Liu, and F. Tufvesson, "Antenna selection in measured massive MIMO channels using convex optimization," in *Proc. IEEE Globecom Workshops*, Atlanta, GA, USA, Dec. 2013, pp. 129–134.

[9] X. Gao, O. Edfors, F. Tufvesson, and E. G. Larsson, "Massive MIMO in real propagation environments: Do all antennas contribute equally?" *IEEE Trans. Commun.*, vol. 63, no. 11, pp. 3917–3928, Nov. 2015.

[10] C. Zhou, Y. Gu, S. He, and Z. Shi, "A robust and efficient algorithm for coprime array adaptive beamforming,"Âİ *IEEE Trans. Veh. Technol.*, vol. 67, no. 2, pp. 1099–1112, Feb. 2018.

[11] A. Alkhateeb, Y.-H. Nam, J. Zhang, and R. W. Heath, Jr., "Massive MIMO combining with switches," *IEEE Wireless Commun. Lett.*, vol. 5, no. 3, pp. 232–235, Jun. 2016.

[12] R. Méndez-Rial, C. Rusu, N. González-Prelcic, A. Alkhateeb, and R. W. Heath, Jr., "Hybrid MIMO architectures for millimeter wave communications: Phase shifters or switches?" *IEEE Access*, vol. 4, pp. 247–267, 2016.

[13] A. Garcia-Rodriguez, C. Masouros, and P. Rulikowski, "Reduced switching connectivity for large scale antenna selection," *IEEE Trans. Commun.*, vol. 65, no. 5, pp. 2250–2263, May 2017.

[14] S. Payami, N. M. Balasubramanya, C. Masouros, and M. Sellathurai, "Phase shifters versus switches: An energy efficiency perspective on hybrid beamforming," *IEEE Wireless Commun. Lett.*, vol. 8, no. 1, pp. 13–16, Feb. 2019.

[15] A. Gorokhov, "Antenna selection algorithms for MEA transmission systems," in *Proc. IEEE Int. Conf. Acoust. Speech Signal Process.*, Orlando, FL, USA, May 2002, pp. 2857–2860.

[16] M. Gharavi-Alkhansari and A. B. Gershman, "Fast antenna subset selection in MIMO systems," *IEEE Trans. Signal Process.*, vol. 52, no. 2, pp. 339–347, Feb. 2004.

[17] A. Dua, K. Medepalli, and A. J. Paulraj, "Receive antenna selection in MIMO systems using convex optimization," *IEEE Trans. Wireless Commun.*, vol. 5, no. 9, pp. 2353–2357, Sep. 2006.

[18] K. Elkhalil, A. Kammoun, T. Y. Al-Naffouri, and M.-S. Alouini, "A blind antenna selection scheme for single-cell uplink massive MIMO," in *Proc. IEEE Globecom Workshops*, Dec. 2016, pp. 1–6.

[19] S. Mahboob, R. Ruby, and V. Leung, "Transmit antenna selection for downlink transmission in a massively distributed antenna system using convex optimization," in *Proc. Int. Conf. Broadband, Wireless Comput. Commun. Appl. (BWCCA)*, Nov. 2012, pp. 228–233.

[20] S. Joshi and S. Boyd, "Sensor selection via convex optimization," *IEEE Trans. Signal Process.*, vol. 57, no. 2, pp. 451–462, Feb. 2009.

[21] I. Berenguer, X. Wang, and V. Krishnamurthy, "Adaptive MIMO antenna selection," in *Proc. 37nth Asilomar Conf. Signals, Syst. Comput.*, Pacific Grove, CA, USA, Nov. 2003, pp. 21–26.

[22] I. Berenguer, X. Wang, and V. Krishnamurthy, "Adaptive MIMO antenna selection via discrete stochastic optimization," *IEEE Trans. Signal Process.*, vol. 53, no. 11, pp. 4315–4329, Nov. 2005.

[23] O. Mehanna, N. D. Sidiropoulos, and G. B. Giannakis, "Joint multicast beamforming and antenna selection," *IEEE Trans. Signal Process.*, vol. 61, no. 10, pp. 2660–2674, May 2013.

[24] O. T. Demir and T. E. Tuncer, "Multicast beamforming with antenna selection using exact penalty approach," in *Proc. IEEE Int. Conf. Acoust., Speech Signal Process. (ICASSP)*, Brisbane, QLD, Australia, Apr. 2015, pp. 2489–2493.

[25] S. He, Y. Huang, J. Wang, L. Yang, and W. Hong, "Joint antenna selection and energy-efficient beamforming design," *IEEE Signal Process. Lett.*, vol. 23, no. 9, pp. 1165–1169, Sep. 2016.

[26] X. Wang and J. Sheng, "Joint antenna selection and beamforming algorithms for physical layer multicasting with massive antennas," *Algorithms*, vol. 9, no. 2, pp. 1–9, Jun. 2016.

[27] J. F. de Andrade, Jr, M. L. R. de Campos, and J. A. Apolinário, Jr., "L_1-constrained normalized LMS algorithms for adaptive beamforming," *IEEE Trans. Signal Process.*, vol. 63, no. 24, pp. 6524–6539, Dec. 2015.

[28] J. F. de Andrade, Jr., M. L. R. de Campos, and J. A. Apolinário Jr., "Sparse solutions for antenna arrays," in *Proc. 29th Simpósio Brasileiro Telecomunicações (SBrT)*, Curitiba, Brazil, Oct. 2011, pp. 1–5.

[29] J. F. de Andrade, Jr, M. L. R. de Campos, and J. A. Apolinário, Jr., "An L_1-constrained normalized LMS algorithm and its application to thinned adaptive antenna arrays," in *Proc. IEEE Int. Conf. Acoust., Speech Signal Process. (ICASSP)*, Vancouver, BC, Canada, May 2013, pp. 3806–3810.

[30] W. Shi, Y. Li, L. Zhao, and X. Liu, "Controllable sparse antenna array for adaptive beamforming," *IEEE Access*, vol. 7, pp. 6412–6423, 2019.

[31] O. L. Frost, III, "An algorithm for linearly constrained adaptive array processing," *Proc. IEEE*, vol. 60, no. 8, pp. 926–935, Aug. 1972.

[32] J. A. Apolinário, S. Werner, P. S. R. Diniz, and T. I. Laakso, "Constrained normalized adaptive filters for CDMA mobile communications," in *Proc. 9th Eur. Signal Process. Conf. (EUSIPCO)*, Rhodes, Greece, Sep. 1998, pp. 2050–2053.

[33] J. C. Bezdek and R. J. Hathaway, "Two new convergence results for alternating optimization," in *Computational Intelligence: The Experts Speak*, D. B. Fogel and C. J. Robinson, Eds. Piscataway, NJ, USA: IEEE Press, 2003, pp. 149–164.

[34] P. S. R. Diniz, *Adaptive Filtering*. Boston, MA, USA: Springer, 2013.

[35] J. Jose, A. Ashikhmin, T. L. Marzetta, and S, Vishwanath, "Pilot contamination and precoding in multi-cell TDD systems," *IEEE Trans. Wireless Commun.*, vol. 10, no. 8, pp. 2640–2651, Aug. 2011.

[36] B. Hassibi and B. M. Hochwald, "How much training is needed in multiple-antenna wireless links?" *IEEE Trans. Inf. Theory*, vol. 49, no. 4, pp. 951–963, Apr. 2003.

[37] S. Noh, M. D. Zoltowski, and D. J. Love, "Training sequence design for feedback assisted hybrid beamforming in massive MIMO systems," *IEEE Trans. Commun.*, vol. 64, no. 1, pp. 187–200, Jan. 2016.

[38] J. A. Zhang, T. Yang, and Z. Chen, "Under-determined training and estimation for distributed transmit beamforming systems," *IEEE Trans. Wireless Commun.*, vol. 12, no. 4, pp. 1936–1946, Apr. 2013.

[39] S. Boyd and L. Vandenberghe, *Convex Optimization*. Cambridge, U.K.: Cambridge Univ. Press, 2004.

GUILHERME MARTIGNAGO ZILLI (S'19) received the B.S. degree in electrical engineering from Santa Catarina State University, Joinville, Brazil, in 2014, and the M.Sc. degree from the Federal University of Santa Catarina, Florianópolis, Brazil, in 2016. He is currently pursuing the Ph.D. degree in electrical engineering with Concordia University, Montreal, QC, Canada. His research interests include signal processing and wireless communications, with emphasis on adaptive algorithms for phased antenna arrays.

Mr. Zilli was a recipient of the Doctoral Research Scholarship Program for Foreign Students, from the Fonds de recherche du Québec—Nature et technologies (FRQNT) and the Concordia International Tuition Award of Excellence.

CIRO ANDRÉ PITZ received the B.S. degree in telecommunication engineering and the M.Sc. degree in electrical engineering from the Regional University of Blumenau, Brazil, in 2008 and 2010, respectively, and the Ph.D. degree in electrical engineering from the Federal University of Santa Catarina, Brazil, in 2015. From 2015 to 2017, he was a Postdoctoral Researcher with the LINSE–Circuits and Signal Processing Laboratory, Federal University of Santa Catarina, Brazil, where he joined the Department of Control, Automation and Computational Engineering, in 2018 and he is currently a Professor. His current research interest includes adaptive signal processing theory and its application in communication systems.

EDUARDO LUIZ ORTIZ BATISTA (S'07–M'10) received the B.S., M.Sc., and Ph.D. degrees from the Federal University of Santa Catarina, Florianópolis, Brazil, in 2002, 2004, and 2009, respectively, all in electrical engineering. Since 2010, he has been with the Federal University of Santa Catarina, where he is currently a Professor, and he is also with the LINSE–Circuits and Signal Processing Laboratory. His current research interests include nonlinear adaptive filtering, reduced-complexity adaptive algorithms, beamforming algorithms, active vibration control, and the statistical analysis of adaptive filters.

RUI SEARA (M'93–SM'04) received the B.S. and M.Sc. degrees in electrical engineering from the Federal University of Santa Catarina, Brazil, in 1975 and 1980, respectively, and the Ph.D. degree in electrical engineering from Paris-Sud University, Paris, France, in 1984. He joined the Electrical Engineering Department, Federal University of Santa Catarina, Brazil, in 1976, where he is currently a Professor of electrical engineering and the Director of the LINSE–Circuits and Signal Processing Laboratory. His research interests include digital and analog filtering, adaptive signal processing algorithms, image and speech processing, and digital communications.

WEI-PING ZHU (SM'97) received the B.E. and M.E. degrees from the Nanjing University of Posts and Telecommunications, in 1982 and 1985, respectively, and the Ph.D. degree from Southeast University, Nanjing, China, in 1991, all in electrical engineering. He was a Postdoctoral Fellow, from 1991 to 1992 and a Research Associate, from 1996 to 1998 with the Department of Electrical and Computer Engineering, Concordia University, Montreal, Canada. From 1993 to 1996, he was an Associate Professor with the Department of Information Engineering, Nanjing University of Posts and Telecommunications. From 1998 to 2001, he was with hi-tech companies in Ottawa, Canada, including Nortel Networks and SR Telecom, Inc. Since July 2001, he has been with the Electrical and Computer Engineering Department, Concordia University, as a full-time Faculty Member, where he is currently a Full Professor. His research interests include digital signal processing fundamentals, speech and statistical signal processing, and signal processing for wireless communication with a particular focus on MIMO systems and cooperative communication.

Dr. Zhu served as an Associate Editor for the IEEE TRANSACTIONS ON CIRCUITS AND SYSTEMS PART I: FUNDAMENTAL THEORY AND APPLICATIONS, from 2001 to 2003, an Associate Editor for *Circuits, Systems and Signal Processing*, from 2006 to 2009, and an Associate Editor for the IEEE TRANSACTIONS ON CIRCUITS AND SYSTEMS PART II: TRANSACTIONS BRIEFS, from 2011 to 2015. He was also a Guest Editor of the IEEE JOURNAL ON SELECTED AREAS IN COMMUNICATIONS for the special issues of: Broadband Wireless Communications for High Speed Vehicles, and Virtual MIMO, from 2011 to 2013. He is currently an Associate Editor of the *Journal of The Franklin Institute*. He was the Secretary of the Digital Signal Processing Technical Committee (DSPTC) of the IEEE Circuits and System Society during June 2012 to May 2014, and the Chair of the DSPTC, from June 2014 to May 2016.